

MKPH-T-97-16
 FTUV/97-41; IFIC/97-41
 Submitted to Phys. Rev. C

Polarization Phenomena in Small-Angle Photoproduction of e^+e^- Pairs and the Gerasimov–Drell–Hearn Sum Rule

A.I. L'vov

P.N. Lebedev Physical Institute, Moscow, 117924, Russia

S. Scopetta*

*Department of Physics, University of Perugia, I-06100 Perugia, Italy
 Institut für Kernphysik, Universität Mainz, D-55099 Mainz, Germany*

D. Drechsel and S. Scherer

Institut für Kernphysik, Universität Mainz, D-55099 Mainz, Germany

(July 1997)

Abstract

Photoproduction of e^+e^- pairs at small angles is investigated as a tool to determine the functions f_1 and f_2 entering the real-photon forward Compton scattering amplitude. The method is based on an interference of the Bethe–Heitler and the virtual Compton scattering mechanisms, generating an azimuthal asymmetry in the e^+ versus e^- yield. The general case of a circularly polarized beam and a longitudinally polarized target allows one to determine both the real and imaginary parts of f_1 as well as f_2 . The imaginary part of f_2 requires target polarization only. We calculate cross sections and asymmetries of the reaction $p(\gamma, e^+e^-)p$, estimate corrections and backgrounds, and propose suitable kinematical regions to perform the experiment. Our investigation shows that photoproduction of e^+e^- -pairs off the proton and light nuclei may serve as a rather sensitive test of the validity of the Gerasimov–Drell–Hearn sum rule.

13.60.Fz, 13.88.+e

Typeset using REVTeX

*Present address: Departament de Física Teòrica, Universitat de València, 46100 Burjassot (València), Spain

I. INTRODUCTION

In studies of spin-dependent structure functions of nucleons and nuclei with real and virtual photons, the verification of the Gerasimov–Drell–Hearn sum rule (GDH) [1,2] is of special interest [3,4]. Apart from general principles as gauge and Lorentz invariance, unitarity, analyticity, and crossing symmetry, this sum rule is based on the assumption that the forward Compton scattering becomes spin independent at high energies. Therefore, the GDH provides an excellent test of the spin dynamics of the nucleon.

In the lab frame, the amplitude for forward Compton scattering off a spin-1/2 target is described by two even functions $f_{1,2}$ of the initial-photon energy ω ,

$$f = \boldsymbol{\epsilon}'^* \cdot \boldsymbol{\epsilon} f_1(\omega) + i\omega \boldsymbol{\sigma} \cdot \boldsymbol{\epsilon}'^* \times \boldsymbol{\epsilon} f_2(\omega), \quad (1)$$

which, at $\omega = 0$, are constrained by the low-energy theorems [5,6]:

$$f_1(0) = -\frac{\alpha Z^2}{M}, \quad f_2(0) = -\frac{\alpha \kappa^2}{2M^2}. \quad (2)$$

Here, M , eZ , and κ are the mass, electric charge, and anomalous magnetic moment of the target, respectively, and $\alpha = e^2/4\pi \simeq 1/137$. Within the framework of the Regge pole model [7,8], these functions behave like

$$f_1(\omega) \propto \omega^{\alpha_R(0)}, \quad f_2(\omega) \propto \omega^{\alpha_R(0)-1} \quad \text{for } \omega \rightarrow \infty, \quad (3)$$

where $\alpha_R(0)$ is the intercept of the leading t -channel Regge exchange contributing to the amplitudes. With the usual assumption of $\alpha_R(0) \lesssim 1$, both f_1 and f_2 satisfy *once*-subtracted dispersion relations. The optical theorem allows one to express the imaginary parts of these amplitudes in terms of the total photoabsorption cross sections $\sigma_{1/2}$ and $\sigma_{3/2}$, where the subscripts refer to total helicities 1/2 and 3/2, respectively,

$$\text{Im } f_1 = \frac{\omega}{8\pi}(\sigma_{1/2} + \sigma_{3/2}) = \frac{\omega}{4\pi}\sigma_{\text{tot}}, \quad \text{Im } f_2 = \frac{1}{8\pi}(\sigma_{1/2} - \sigma_{3/2}) \equiv \frac{1}{4\pi}\Delta\sigma. \quad (4)$$

Therefore, we may write dispersion relations for f_1 and f_2 ,

$$f_1(\omega) = -\frac{\alpha Z^2}{M} + \frac{\omega^2}{2\pi^2} \int_{\omega_{\text{thr}}}^{\infty} \frac{\sigma_{\text{tot}}(\omega')}{\omega'^2 - \omega^2 - i0^+} d\omega', \quad (5)$$

$$f_2(\omega) = -\frac{\alpha \kappa^2}{2M^2} + \frac{\omega^2}{2\pi^2} \int_{\omega_{\text{thr}}}^{\infty} \frac{\Delta\sigma(\omega')}{\omega'^2 - \omega^2 - i0^+} \frac{d\omega'}{\omega'}. \quad (6)$$

The GDH,

$$\int_{\omega_{\text{thr}}}^{\infty} (\sigma_{3/2}(\omega) - \sigma_{1/2}(\omega)) \frac{d\omega}{\omega} = \frac{2\pi^2 \alpha \kappa^2}{M^2}, \quad (7)$$

arises from Eq. (6) under the stronger assumption that $f_2(\omega) \rightarrow 0$ for $\omega \rightarrow \infty$, or alternatively $\alpha_R(0) < 1$. Numerical investigations [9–12] of the integral on the lhs of Eq. (7) in

the case of the nucleon reveal a different behavior for the two isospin combinations of the proton and neutron amplitudes,

$$f_{1,2}^{I=0} = \frac{1}{2}(f_{1,2}^p + f_{1,2}^n), \quad f_{1,2}^{I=1} = \frac{1}{2}(f_{1,2}^p - f_{1,2}^n), \quad (8)$$

which correspond to isoscalar and isovector exchanges in the t -channel. The GDH for $I = 0$ seems to work very successfully, supporting the conjecture that the leading isoscalar Regge exchange (Pomeron) is decoupled from the spin-dependent transitions. It is very surprising, however, that the GDH for $I = 1$ seems to be violated, despite the fact that all known isovector exchanges (such as the a_1 and a_2 mesons) have an intercept $\alpha_R(0) \lesssim 0.5$ which supports the assumption of $f_2^{I=1} \rightarrow 0$ for $\omega \rightarrow \infty$.

As was emphasized in [12], the scale of the violation in the isovector sector is not small. Evaluating the GDH integral, Eq. (7), with the VPI multipoles for single-pion photoproduction (solution SP97K [13]) and with the model of Ref. [14] for double-pion photoproduction, up to the energy of 1 GeV we find for the $I = 1$ component

$$38.8 + 8.0 = 46.8 \mu\text{b} \quad (\text{GDH } I = 1, \omega \leq 1 \text{ GeV}), \quad (9)$$

which has to be compared with $-14.2 \mu\text{b}$ of the rhs of Eq. (7). In Eq. (9), the 1π - and 2π -contributions are given separately. Analogously, we obtain for the $I = 0$ component of the GDH

$$164.6 + 52.9 = 217.5 \mu\text{b} \quad (\text{GDH } I = 0, \omega \leq 1 \text{ GeV}), \quad (10)$$

which matches the value $218.9 \mu\text{b}$ of the rhs of Eq. (7). The large positive 2π contribution in Eq. (10) is related with the process $\gamma N \rightarrow \pi\Delta$ which is predominantly isovector and contributes little to Eq. (9). Assuming that the difference between Eq. (9) and the GDH prediction is resolved by an excess of the neutron over the proton cross section at higher energies, e.g., between 1 to 3 GeV, we would obtain $(\sigma_{3/2} - \sigma_{1/2})^n - (\sigma_{3/2} - \sigma_{1/2})^p \simeq 110 \mu\text{b}$. Such a huge difference would be a great surprise, because the total cross section is $\sigma_{\text{tot}} \simeq 120\text{--}150 \mu\text{b}$ at these energies.

We can think of two options to explain the discrepancy.

1. The GDH for $I = 1$ is not valid, and we have the first experimentally established example that the high-energy behavior of a photon scattering amplitude is determined by the so-called fixed pole ($J = 1$) in the complex plane of the angular momentum [7] rather than known Regge exchanges with smaller intercepts $\alpha_R(0)$. In particular, this would violate the assumption of Vector Meson Dominance in high-energy Compton scattering since fixed poles are forbidden in vector meson photoproduction [7]. Some arguments against the fixed pole are discussed in [4].
2. The existing experimental information on the spin and isospin dependence of photoabsorption is not accurate enough. An alternative experiment to clarify the nature of the discrepancy would be to measure the amplitude $f_2(\omega)$, Eq. (6).

A straightforward way to study $\text{Im } f_2$ is provided by measuring the photoproduction cross sections $\sigma_{1/2}$ and $\sigma_{3/2}$ over a wide energy region, using 4π detectors for the final hadrons. An

independent determination of $\text{Re } f_2$ by photon scattering would also be of interest since it constrains the high-energy behavior of $\Delta\sigma$ via the dispersion relation, Eq. (6). In the present paper we propose an alternative method to determine both $\text{Re } f_2$ and $\text{Im } f_2$ by measuring the photoproduction of small-angle e^+e^- pairs which serve as a polarimeter of the virtual photon in the subprocess

$$\gamma N \rightarrow \gamma^* N'. \quad (11)$$

Since the conversion factor of the virtual photon into the e^+e^- pairs is small ($\sim \alpha/3\pi$), this contribution will be strongly suppressed compared with a huge background of Bethe-Heitler (BH) pair production. However, the interference between the Bethe-Heitler amplitude and the amplitude of virtual Compton scattering (VCS) leads to a specific azimuthal asymmetry between yields of positrons and electrons which could be studied with polarized photons and targets. A similar method was already used in Ref. [15] to determine $\text{Re } f_1$ at an energy of 2.2 GeV using an unpolarized beam and an unpolarized target.

II. BETHE–HEITLER AND VIRTUAL COMPTON SCATTERING AMPLITUDES

Considering the reaction

$$\gamma N \rightarrow e^+ e^- N' \quad (12)$$

in the lab frame, we denote the energy, momentum, and helicity of the positron by ε_1 , \mathbf{p}_1 , $\frac{1}{2}h_1$. Similarly, we use ε_2 , \mathbf{p}_2 , $\frac{1}{2}h_2$ for the kinematical variables of the electron and ω , \mathbf{k} , h_γ for the photon. The nucleon spin projections on the direction of the photon beam are denoted by $\frac{1}{2}h_N$ and $\frac{1}{2}h'_N$, and the masses of the nucleon and leptons by M and m , respectively.

Aside from an overall azimuthal angle, the kinematics of e^+e^- photoproduction is specified by four variables. We choose two of them to be the invariant mass W of the pair and the invariant momentum transfer Q ,

$$W^2 = k'^2, \quad k' \equiv p_1 + p_2, \quad Q^2 = -q^2, \quad q \equiv p'_N - p_N. \quad (13)$$

The beam direction $\hat{\mathbf{k}}$ and the vector \mathbf{k}' define the reaction plane. Furthermore, we introduce the fractions of the virtual-photon energy ω' , which are carried by the positron and electron, respectively,

$$x_1 = \frac{\varepsilon_1}{\omega'}, \quad x_2 = \frac{\varepsilon_2}{\omega'} = 1 - x_1, \quad \omega' = \varepsilon_1 + \varepsilon_2, \quad (14)$$

and denote the azimuthal angles of the two particles, with respect to the total momentum \mathbf{k}' of the pair and the reaction plane, by ϕ_1 and $\phi_2 = \pi + \phi_1$ (see Fig. 1). The kinetic energy and momentum of the recoiling nucleon read

$$q_0 = \frac{Q^2}{2M}, \quad q_z = q_0 + \frac{W^2 + Q^2}{2\omega}, \quad q_\perp^2 = Q^2 + q_0^2 - q_z^2 \geq 0, \quad (15)$$

where the z -axis is directed along the photon beam. The energy and momentum carried by the pair are $\omega' = \omega - q_0$ and $\mathbf{k}' = \mathbf{k} - \mathbf{q}$, respectively. The polar angles between $\mathbf{p}_{1,2}$ and \mathbf{k}' are given by

$$2|\mathbf{p}_i| |\mathbf{k}'| \cos \theta_i = 2\varepsilon_i \omega' - W^2, \quad i = 1, 2, \quad (16)$$

and the angle θ between the beam and the total momentum of the pair follows from

$$\tan \theta = \frac{q_\perp}{\omega - q_z}. \quad (17)$$

The differential cross section of reaction (12) reads

$$d\sigma = \frac{1}{(4\pi)^3} \frac{\omega'}{|\mathbf{k}'|} \frac{dW^2 dQ^2}{16M^2\omega^2} dx_1 \frac{d\phi_1}{2\pi} |T|^2, \quad (18)$$

where the appropriate sum or average over spin projections is implied.

To lowest order in the electromagnetic coupling $e > 0$, the amplitude $T = T_{\text{BH}} + T_{\text{VCS}}$ consists of the contributions shown in Fig. 2. Typically, we consider the kinematical region of

$$\omega \simeq 1 \text{ GeV}, \quad W \simeq 50 \text{ MeV}, \quad Q \simeq 100 \text{ MeV}, \quad x_1 \simeq x_2 \simeq 0.5, \quad (19)$$

corresponding to small angles $p_{1\perp}/\varepsilon_1 \ll 1$ and $p_{2\perp}/\varepsilon_2 \ll 1$ between the photon beam and the momenta of the leptons. We also assume that $p_{1\perp}, p_{2\perp} \gg m$. In this region the angles θ_i ,

$$\sin^2 \theta_i = \frac{1}{\mathbf{k}'^2 \mathbf{p}_i^2} \left[\varepsilon_1 \varepsilon_2 W^2 - m^2 \mathbf{k}'^2 - \frac{W^4}{4} \right] \simeq \frac{W^2}{\omega^2} \left(\frac{1}{x_i} - 1 \right), \quad (20)$$

are proportional to the invariant mass W , and the total opening angle of the pair is equal to

$$\theta_1 + \theta_2 \simeq \frac{W}{\omega} (x_1 x_2)^{-1/2}. \quad (21)$$

The BH amplitude is

$$T_{\text{BH}} = -\frac{e^3 J^\mu}{Q^2} \bar{u}(p_2, h_2) \left[\gamma_\mu \frac{\gamma \cdot (k - p_1) + m}{(k - p_1)^2 - m^2} \gamma \cdot \epsilon + \gamma \cdot \epsilon \frac{\gamma \cdot (p_2 - k) + m}{(p_2 - k)^2 - m^2} \gamma_\mu \right] v(p_1, h_1), \quad (22)$$

where ϵ_μ is the photon polarization vector and J_μ is the nucleon electromagnetic current,

$$J_\mu = \bar{u}'(h'_N) \left\{ \gamma_\mu F_1(t) + \frac{1}{4M} [\gamma \cdot q, \gamma_\mu] F_2(t) \right\} u(h_N), \quad (23)$$

with $t = -Q^2$ and the form factors normalized to $F_1(0) = Z$ and $F_2(0) = \kappa$.

In the case of particles with definite helicities we follow the phase conventions of Jacob and Wick (see, e.g., [16,17]),

$$\epsilon = (0; \boldsymbol{\epsilon}) = \frac{1}{\sqrt{2}} (0; -h_\gamma, -i, 0), \quad (24)$$

and

$$u(p_2, h_2) = \begin{pmatrix} \sqrt{\varepsilon_2 + m} \\ h_2 \sqrt{\varepsilon_2 - m} \end{pmatrix} \chi(p_2, h_2), \quad v(p_1, h_1) = \begin{pmatrix} -\sqrt{\varepsilon_1 - m} \\ h_1 \sqrt{\varepsilon_1 + m} \end{pmatrix} \chi(p_1, -h_1). \quad (25)$$

Here $\chi(p, h)$ are Pauli spinors with helicity $\frac{1}{2}h$,

$$\chi(p, +) = \frac{1}{\sqrt{2p(p+p_z)}} \begin{pmatrix} p+p_z \\ p_x + ip_y \end{pmatrix}, \quad \chi(p, -) = \frac{1}{\sqrt{2p(p+p_z)}} \begin{pmatrix} -p_x + ip_y \\ p+p_z \end{pmatrix}. \quad (26)$$

For the nucleon polarized along the z -axis we have

$$u(h_N) = \sqrt{2M} \begin{pmatrix} 1 \\ 0 \end{pmatrix} X(h_N), \quad u'(h'_N) = \frac{1}{\sqrt{2M+q_0}} \begin{pmatrix} 2M+q_0 \\ \boldsymbol{\sigma} \cdot \mathbf{q} \end{pmatrix} X(h'_N), \quad (27)$$

where

$$X(+)=\begin{pmatrix} 1 \\ 0 \end{pmatrix}, \quad X(-)=\begin{pmatrix} 0 \\ 1 \end{pmatrix}. \quad (28)$$

Using these formulae we compute the amplitude T_{BH} for the appropriate polarizations of all 5 particles. For high energies and small angles of the produced leptons, we obtain a good approximation by neglecting the lepton mass in Eqs. (22) and (25) and the q/M terms in Eqs. (23) and (27), and replacing p_z by p in Eq. (26). Keeping the leading terms in the transverse momenta, we arrive at the simple formula

$$T_{\text{BH}} \simeq -\frac{4Me^3 F_1(t)}{Q^2} \omega \sqrt{x_1 x_2} (x_1 - x_2 + h_1 h_\gamma) \boldsymbol{\epsilon} \cdot \mathbf{D} \delta_{h_1, -h_2} \delta_{h_N, h'_N}, \quad (29)$$

with

$$\mathbf{D} = \frac{\mathbf{p}_{1\perp}}{p_{1\perp}^2} + \frac{\mathbf{p}_{2\perp}}{p_{2\perp}^2} \quad (30)$$

and

$$\begin{aligned} p_{1\perp}^2 &\simeq x_1^2 Q^2 + 2x_1 \sqrt{x_1 x_2} W Q \cos \phi_1 + x_1 x_2 W^2, \\ p_{2\perp}^2 &\simeq x_2^2 Q^2 - 2x_2 \sqrt{x_1 x_2} W Q \cos \phi_1 + x_1 x_2 W^2. \end{aligned} \quad (31)$$

In the kinematics of Eq. (19), Eq. (29) agrees within 1–2% with the full calculation of the largest matrix elements ($h_1 = -h_2$, $h_N = h'_N$). The nucleon-spin-flip amplitudes which are not described by the approximation (29) are suppressed by a factor Q/M . They contribute incoherently to the differential cross section summed over the final polarizations, and their contribution is only $\simeq 2\%$ at $Q = 100$ MeV. The amplitudes with $h_1 = h_2$ are suppressed by $m/p_{1,2\perp}$, and their incoherent contribution is completely negligible except for the region of very small $p_{1,2\perp}$ of about a few MeV which is beyond the scope of our consideration.

Next we consider the amplitude

$$T_{\text{VCS}} = \frac{e}{W^2} \epsilon^\mu T_{\mu\nu} l^\nu, \quad (32)$$

where

$$l_\nu = \bar{u}(p_2)\gamma_\nu v(p_1) \quad (33)$$

is the lepton current. $T_{\mu\nu}$ is the amplitude of the subprocess (11), which is generally described by 12 functions [18] of the photon energy ω , the scattering angle θ , and the virtual photon mass W . We assume, however, that $T_{\mu\nu}$ at small angles and photon masses can be approximated by Eq. (1), i.e. by forward scattering of real photons. Corrections to this approximation arise from (i) longitudinal photon polarization, (ii) finite photon mass, and (iii) $\theta \neq 0$. We briefly discuss these effects in order.

(i) Using gauge invariance of the amplitude $M_\nu \equiv \epsilon^\mu T_{\mu\nu}$, i.e. $M^\nu k'_\nu = 0$, and current conservation, $l^\nu k'_\nu = 0$, we express the time-like components of M_ν and l_ν by the longitudinal ones (along $\hat{\mathbf{k}}'$),

$$M^\nu l_\nu \equiv M_0 l_0 - M_L l_L - \mathbf{M}_T \cdot \mathbf{l}_T = -\frac{W^2}{\omega'^2} M_L l_L - \mathbf{M}_T \cdot \mathbf{l}_T. \quad (34)$$

Obviously, the longitudinal contribution vanishes for real photons, $W^2 \rightarrow 0$. To get a more quantitative estimate, we note that the space-like components of the lepton current, Eq. (33), are given in the small-angle approximation by

$$l_L \simeq -2\omega\sqrt{x_1 x_2} \delta_{h_1, -h_2} \quad (35)$$

and

$$\mathbf{l}_T \simeq \sqrt{x_1 x_2} \delta_{h_1, -h_2} \left[(x_1 - x_2) \mathbf{d} - i h_1 \hat{\mathbf{k}} \times \mathbf{d} \right], \quad (36)$$

where

$$\mathbf{d} = \frac{\mathbf{p}_{1\perp}}{x_1} - \frac{\mathbf{p}_{2\perp}}{x_2} \quad (37)$$

is directed perpendicular to the photon beam. (Note that the subscript \perp denotes orthogonality to the z -axis, the subscript T orthogonality to the direction of $\hat{\mathbf{k}}'$). Since the BH amplitude is essentially independent of the nucleon spin, see Eq. (29), the interference of T_{BH} and T_{VCS} is dominated by the no-spin-flip terms in M_L and \mathbf{M}_T . Due to angular momentum conservation in the transition $\gamma(h_\gamma = \pm 1)N \rightarrow \gamma^*(h = 0)N$, the no-spin-flip part of M_L has to vanish like θ for small angles. As a toy model, we may consider Compton scattering through E1-excitation followed by the decay of a resonance with the quantum numbers of the $D_{13}(1520)$. The corresponding amplitude $\epsilon_\mu T^{\mu\nu} \epsilon'_\nu$ is proportional to

$$\epsilon'^* \cdot \mathbf{S}^+ \boldsymbol{\epsilon} \cdot \mathbf{S} = \frac{2}{3} \epsilon'^* \cdot \boldsymbol{\epsilon} - \frac{i}{3} \boldsymbol{\sigma} \cdot \boldsymbol{\epsilon}'^* \times \boldsymbol{\epsilon} = \frac{2 + h_\gamma h_N}{3} \boldsymbol{\epsilon}'^* \cdot \boldsymbol{\epsilon}, \quad (38)$$

where \mathbf{S} is the transition spin operator (see, e.g. [19]) and $\boldsymbol{\sigma}$ is the nucleon spin operator, which can be replaced by $h_N \hat{\mathbf{k}}$ for no-spin-flip transitions. Accordingly, in such transitions the amplitude $\epsilon_i T_{ij} \epsilon'_j$ is proportional to $\boldsymbol{\epsilon}'^* \cdot \boldsymbol{\epsilon}$, and the L/T ratio reads

$$\frac{|M_L|}{|\mathbf{M}_T|} = \frac{1}{\sqrt{2}} \sin \theta \simeq \frac{Q}{\omega\sqrt{2}}. \quad (39)$$

To be more accurate, we should do this calculation in the rest frame of the resonance rather than in the lab frame. However, such a calculation does not change too much the estimate (39).

Using the relationship

$$\mathbf{d}^2 \simeq (x_1 x_2)^{-1} W^2, \quad (40)$$

valid at high energies and small angles, we finally conclude that the longitudinal contribution of M_L to Eq. (34) is smaller than the contribution of M_T by a factor $\simeq WQ/\omega^2$, which is typically $\lesssim 1\%$ in the kinematics of Eq. (19).

It is worth noting that the longitudinal contribution in Eq. (34) does not depend on the azimuthal direction of the vector \mathbf{d} , and its interference with T_{BH} does not contribute to azimuthal variations of positron and electron yields. The longitudinal contribution leads only to a small change of the cross sections and asymmetries.

(ii) Another consequence of the virtuality of the photon γ^* in the subprocess (11) is the presence of additional form factors at the photon-baryon vertices. We may expect that such form factors would increase the amplitude T_{VCS} by a factor $\simeq W^2/m_\rho^2$ which is $\lesssim 1\%$ for the kinematics considered.

(iii) In the general case of $\theta \neq 0$, the amplitude for real Compton scattering is characterized by 6 independent functions $A_i(\omega, \theta)$. Even for no-spin-flip transitions we still have 4 different amplitudes (see Appendix A). Two of them describe no-photon-helicity-flip transitions and manifest themselves in the amplitude T_{VCS} exactly like the functions f_1 and f_2 except for an additional angular dependence. The other two, \tilde{f}_1 and \tilde{f}_2 , vanish at $\theta = 0$ and describe photon scattering involving a helicity flip. They result in a different azimuthal structure of the BH-VCS interference, and give rise to $\cos 2\phi$ and $\sin 2\phi$ corrections to the formula discussed in the next section.

The simple dipole model of Eq. (38) suggests that the angular dependence of f_1 and f_2 follows $1 + \cos \theta$, such that the ($\theta \neq 0$)-corrections are roughly of the scale $\theta^2 \simeq 1\%$. However, already at energies of 1 GeV many higher multipoles contribute and the realistic angular dependence is steeper. In terms of the invariant momentum transfer $t = -Q^2$, the slope $B/2 \simeq 3 \text{ GeV}^{-2}$ of the amplitude $f_1(\omega, t)$ at high energies should be close to the diffractive slope of the differential cross section $d\sigma/dt \propto \exp(Bt)$ of Compton scattering [20]. Thus the decrease of f_1 at $Q \simeq 100 \text{ MeV}$ is $\simeq 3\%$. Nothing definite is known for $f_2(\omega, t)$ and for the flip amplitudes \tilde{f}_1 and \tilde{f}_2 . From dispersion calculations of the amplitudes A_i [14] we find that the amplitude f_1 at $\omega = 1 \text{ GeV}$ decreases by 1.4% and 3.9% (real and imaginary parts, respectively), when t varies from 0 to -0.01 GeV^2 . For the amplitude f_2 the decrease is equal to 0.6% and 5.2%, respectively. At $t = -0.01 \text{ GeV}^2$ the helicity-flip amplitudes are very small, $|\tilde{f}_1/f_1| = 0.3\%$ and $|\tilde{f}_2/f_2| = 0.15\%$. We conclude that even for a momentum transfer Q of 100 MeV the Compton scattering amplitude is not modified by more than $\simeq 5\%$, at least at $\omega = 1 \text{ GeV}$.

Eventually, we evaluate the amplitude T_{VCS} by keeping only the term $-\mathbf{M}_T \cdot \mathbf{l}_T$ in Eq. (34) with

$$-\mathbf{M}_T = 8\pi M \boldsymbol{\epsilon} (f_1 - h_\gamma h_N \omega f_2) \delta_{h_N, h'_N}, \quad (41)$$

where the factor $8\pi M$ provides the correct normalization and the term with f_2 is treated in

the no-spin-flip approximation $\boldsymbol{\sigma} \rightarrow h_N \hat{\mathbf{k}}$. Using Eq. (36), we finally obtain ¹

$$T_{\text{VCS}} \simeq \frac{8\pi Me}{W^2} \sqrt{x_1 x_2} \boldsymbol{\epsilon} \cdot \mathbf{d}(x_1 - x_2 + h_1 h_\gamma) \\ \times \left(f_1(\omega) - h_\gamma h_N \omega f_2(\omega) \right) \delta_{h_1, -h_2} \delta_{h_N, h'_N}. \quad (42)$$

From the above arguments we expect that this approximation to T_{VCS} is sufficient to describe interference effects between the BH and VCS amplitudes with a relative accuracy of a few per cent.

III. AZIMUTHAL ASYMMETRIES AND DETERMINATION OF F_2

Generally, the VCS amplitude, Eq. (42), is small in comparison with the BH amplitude, Eq. (29), and can be seen only through BH–VCS interference which, in turn, can be observed because of a specific signature of odd C -parity of the leptons (C_L parity). Under charge conjugation the lepton pair and the electromagnetic field transform as

$$|e^+(p_1, h_1), e^-(p_2, h_2)\rangle \xrightarrow{C} |e^-(p_1, h_1), e^+(p_2, h_2)\rangle = -|e^+(p_2, h_2), e^-(p_1, h_1)\rangle, \\ A_\mu(x) \xrightarrow{C} -A_\mu(x). \quad (43)$$

Thus the relevant amplitudes for a process where the lepton pair is produced by a *single* virtual photon, e.g. in VCS or in the background reaction

$$\gamma p \rightarrow \pi^0 X \rightarrow e^+ e^- \gamma X, \quad (44)$$

are even under the interchange

$$\varepsilon_1, \mathbf{p}_1, h_1 \leftrightarrow \varepsilon_2, \mathbf{p}_2, h_2. \quad (45)$$

On the other hand, the BH reaction involves the interaction of the pair with *two* photons and, therefore, the BH amplitude is odd under Eq. (45). Thus its interference with the VCS contribution leading to the *same* final state is antisymmetrical under the exchange $1 \leftrightarrow 2$.

The BH cross section, summed over the polarizations of the lepton pair and the recoil proton, has been calculated for various kinematical situations (see, e.g., Fig. 3). It can be directly obtained from the amplitude (29). In order to check the numerical calculations and to obtain simple analytical expressions, the following approximations are useful. We define, as an estimate for the yield,

$$\sigma_{12}^{\text{BH}} \equiv 2\pi W Q \frac{d^4 \sigma^{\text{BH}}}{dW dQ dx_1 d\phi_1} \simeq \frac{8\alpha^3 Z^2 W^2}{Q^2} x_1 x_2 (x_1^2 + x_2^2) \mathbf{D}^2, \quad (46)$$

which is symmetric under $1 \leftrightarrow 2$. Note that

¹In the first report on our calculation [21] the amplitude T_{VCS} was given a wrong sign.

$$\mathbf{D}^2 \simeq \frac{Q^2}{p_{1\perp}^2 p_{2\perp}^2}, \quad (47)$$

where $p_{1,2\perp}^2$ are given in Eq. (31). In the particular case of $x_1 = x_2 = 1/2$,

$$|\mathbf{D}(\phi_1 = \pm \frac{\pi}{2})| \simeq \frac{4Q}{Q^2 + W^2}, \quad |\mathbf{D}(\phi_1 = 0 \text{ or } \pi)| \simeq \frac{4Q}{|Q^2 - W^2|}. \quad (48)$$

In the total cross section, the excess of positrons over electrons at some angles is due to the C_L -odd interference term,

$$\sigma_{12} - \sigma_{21} \approx -\frac{16\alpha^2 Z}{\omega} x_1 x_2 (x_1^2 + x_2^2) |\mathbf{d}| |\mathbf{D}| F(\omega, \phi), \quad (49)$$

where the function

$$F(\omega, \phi) = (\text{Re } f_1(\omega) - h_\gamma h_N \omega \text{Re } f_2(\omega)) \cos \phi \\ + (-h_\gamma \text{Im } f_1(\omega) + h_N \omega \text{Im } f_2(\omega)) \sin \phi \quad (50)$$

depends on the azimuthal angle ϕ between the vectors \mathbf{d} and \mathbf{D} and carries information on the real and imaginary parts of $f_{1,2}$. The azimuth of \mathbf{d} coincides with ϕ_1 , but the vector \mathbf{D} in general does not lie in the reaction plane,

$$\phi = \phi_1 - \phi_D, \quad \sin \phi_D \simeq -\frac{W \sin \phi_1}{p_{1\perp} p_{2\perp}} \left(2x_1 x_2 W \cos \phi_1 + (x_1 - x_2) \sqrt{x_1 x_2} Q \right). \quad (51)$$

In particular, ϕ and ϕ_1 are the same when the pair is symmetric ($x_1 = x_2$), and \mathbf{p}_1 is in the reaction plane ($\phi_1 = 0$ or π , $Q > W$) or transversely to the plane ($\phi_1 = \pm \pi/2$).

The function $F(\omega, \phi)$ can be measured through the e^+e^- asymmetry,

$$\Sigma_{12} = \frac{\sigma_{12} - \sigma_{21}}{\sigma_{12} + \sigma_{21}} \simeq \frac{2 \text{Re} [T_{\text{VCS}} T_{\text{BH}}^*]}{|T_{\text{BH}}|^2} \simeq -\frac{Q^2}{\alpha Z \omega W} \frac{F(\omega, \phi)}{\sqrt{x_1 x_2} |\mathbf{D}|}, \quad (52)$$

provided that background contributions such as (44) are subtracted. The available knowledge of f_1 can be used to test this procedure.

Corresponding to the helicity structure of the function F , we may introduce 4 different asymmetries A , A_γ , A_N , and $A_{\gamma N}$, such that

$$\Sigma_{12} = A + h_\gamma A_\gamma + h_N A_N + h_\gamma h_N A_{\gamma N}. \quad (53)$$

The indices of these coefficients denote which particles are polarized. The asymmetries A and $A_{\gamma N}$ are proportional to $\text{Re } f_1$ and $\text{Re } f_2$, respectively, and can be measured by observing the leptons in the reaction plane. The asymmetries A_γ and A_N are proportional to $\text{Im } f_1$ and $\text{Im } f_2$, respectively, and can be measured by detecting leptons emitted transversely to the reaction plane.

The amplitudes f_1 and f_2 (see Fig. 4) and the asymmetries (see Fig. 5) are estimated by using unitarity (4) and the dispersion relations (5) and (6). The amplitudes $\text{Im } f_1$ and $\text{Re } f_1$ can be reliably calculated on the basis of the total photoabsorption data for the proton [22,23], and the quantity $\Delta\sigma$ has been evaluated by using the model of [14],

accounting for our present knowledge of single-pion photoproduction multipoles [13] and resonance and background mechanisms of double-pion photoproduction. We note that these calculations are only performed in order to illustrate the corrections due to A_N and $A_{\gamma N}$. The asymmetries A and A_γ should be measured and could be used for calibration purposes.

We emphasize that even with unpolarized photons one can measure the GDH cross section $\Delta\sigma \propto \text{Im } f_2$. If the photon hits the target polarized along the beam direction *and* the spin-3/2 photoabsorption cross section $\sigma_{3/2}$ is bigger than $\sigma_{1/2}$, the positron is preferentially emitted to the rhs of the reaction plane (i.e. $\mathbf{k} \times \mathbf{k}' \cdot \mathbf{p}_1 > 0$). The corresponding asymmetry for $x_1 = x_2$,

$$A_N(\phi_1 = \frac{\pi}{2}) \simeq -\frac{Q(Q^2 + W^2)}{8\pi\alpha ZW} \Delta\sigma, \quad (54)$$

is sensitive to $\Delta\sigma$, with a proportionality factor independent of the photon energy. In the kinematics of Eq. (19), a value $\Delta\sigma = \mp 29 \mu\text{b}$ leads to an asymmetry $A_N = \pm 1\%$. Therefore it is necessary to measure A_N with the accuracy $\delta A_N \simeq 10^{-3}$ in order to obtain useful constraints on $\Delta\sigma$.

As can be seen from Eq. (6), the convergence of the GDH integral to its canonical value, Eq. (7), and its saturation by energies $\omega^2 \ll \omega_0^2$, can happen if and only if $f_2(\omega) \ll f_2(0)$ for $\omega \gtrsim \omega_0$. Given, for example, $R \equiv \text{Re } f_2(\omega)/f_2(0) = \pm 5\%$, we expect to see the asymmetry

$$A_{\gamma N}(\phi_1 = 0, x_1 = x_2) = -R \frac{\kappa^2 Q}{4M^2 W} (Q^2 - W^2) = \mp 0.07\% \quad (55)$$

in the kinematics of Eq. (19) independently of ω . Therefore, an experiment determining whether the asymmetries $A_{\gamma N}$ and A_N at energies of a few GeV are less than $\simeq 10^{-3}$ would provide a clean test of the validity of the GDH sum rule at the accuracy level of a few per cent.

Combining the helicity amplitudes (29) and (42) with $h_\gamma = \pm 1$, we obtain cross sections and asymmetries for linearly-polarized photons. Introducing $\mathbf{s} = \hat{\mathbf{k}} \times \boldsymbol{\epsilon}$, we obtain cross sections by substituting, in Eq. (46),

$$(x_1^2 + x_2^2) \mathbf{D}^2 \rightarrow (x_1 - x_2)^2 (\boldsymbol{\epsilon} \cdot \mathbf{D})^2 + (\mathbf{s} \cdot \mathbf{D})^2, \quad (56)$$

and the asymmetry by replacing, in Eq. (49),

$$\begin{aligned} (x_1^2 + x_2^2) |\mathbf{d}| |\mathbf{D}| F(\omega, \phi) &\rightarrow \left[(x_1 - x_2)^2 \boldsymbol{\epsilon} \cdot \mathbf{d} \boldsymbol{\epsilon} \cdot \mathbf{D} + \mathbf{s} \cdot \mathbf{d} \mathbf{s} \cdot \mathbf{D} \right] \text{Re } f_1 \\ &+ \left[(x_1 - x_2)^2 \mathbf{s} \cdot \mathbf{d} \boldsymbol{\epsilon} \cdot \mathbf{D} - \boldsymbol{\epsilon} \cdot \mathbf{d} \mathbf{s} \cdot \mathbf{D} \right] h_N \omega \text{Im } f_2. \end{aligned} \quad (57)$$

As in the case of unpolarized photons, only $\text{Re } f_1$ and $\text{Im } f_2$ can be measured in this way.

For the sake of completeness we mention that the same interference structures exist in the crossed reaction

$$e^- p \rightarrow e^- p \gamma, \quad (58)$$

which recently attracted considerable interest as a tool to study VCS [24]. The corresponding BH and VCS amplitudes in the small-angle approximation are obtained similarly to Eqs. (29) and (42), or via the crossing symmetry $(\varepsilon_1, \mathbf{p}_1, h_1 \rightarrow -\varepsilon, -\mathbf{p}, -h, \varepsilon_2, \mathbf{p}_2, h_2 \rightarrow \varepsilon', \mathbf{p}', h')$,

and $\omega, \boldsymbol{\epsilon}, h_\gamma \rightarrow -\omega, -\boldsymbol{\epsilon}^*, -h_\gamma$; the sign of minus in $\boldsymbol{\epsilon}^*$ is related to the definition of the helical vectors). They are

$$T_{\text{BH}} \simeq \frac{4Me^3 F_1(t)}{-t} \frac{\sqrt{\varepsilon\varepsilon'}}{\omega} (\varepsilon + \varepsilon' + \omega h_\gamma h) \left(-\frac{\boldsymbol{\epsilon}^* \cdot \mathbf{p}}{p_\perp^2} + \frac{\boldsymbol{\epsilon}^* \cdot \mathbf{p}'}{p_\perp'^2} \right) \delta_{h,h'} \delta_{h_N,h'_N}, \quad (59)$$

where the transverse components and the nucleon spin projections are considered with respect to the direction of the final photon momentum \mathbf{k} , and

$$T_{\text{VCS}} \simeq \frac{8\pi Me}{-(p-p')^2} \frac{\sqrt{\varepsilon\varepsilon'}}{\omega} (\varepsilon + \varepsilon' + \omega h_\gamma h) \left(\frac{\boldsymbol{\epsilon}^* \cdot \mathbf{p}}{\varepsilon} - \frac{\boldsymbol{\epsilon}^* \cdot \mathbf{p}'}{\varepsilon'} \right) \times (f_1(\omega) - h_\gamma h_N \omega f_2(\omega)) \delta_{h,h'} \delta_{h_N,h'_N}. \quad (60)$$

However, the important difference is that there is no natural way to measure the C_L -odd effects in the reaction (58), except by using also a positron beam.

IV. YIELDS AND BACKGROUNDS

With regard to an optimal choice of W and Q , we note that the yield estimate of the lepton pairs (cf. (46)) is proportional to $W^2 \mathbf{D}^2 / Q^2$. The statistical fluctuations in the asymmetry, $\delta\Sigma_{12} \propto Q/W|\mathbf{D}|$, are by a factor of Q smaller than the asymmetry, $\Sigma_{12} \propto Q^2/W|\mathbf{D}|$. Thus it is profitable to choose Q as large as possible, keeping Q still small enough to fit the condition imposed by a small scattering angle θ as discussed in the previous section. The choice of W is less important, provided that W is still close enough to the real-photon point. On the other hand, W should not be less than $\simeq 10$ MeV, since otherwise multiple Coulomb scattering of the leptons in the target would prevent an accurate measurement of small transverse momenta.

In the kinematics of Eq. (19), which satisfies all of the above requirements, the BH cross section (46) is a few tens of a nanobarn (see Fig. 3). With an untagged photon beam intensity of $I_\gamma \simeq 10^9 \text{ s}^{-1}$, and a target of density $N \simeq 5 \cdot 10^{23} \text{ cm}^{-2}$, the count rate is expected to reach a few events per second. This should make it possible to measure asymmetries with an accuracy $\simeq 10^{-3}$.

Most of the BH pairs are produced at very forward angles, and the experimental setup should be insensitive to them. The average load of a single lepton detector is determined by the inclusive BH cross section integrated over the directions of the second lepton [25],

$$2\pi p_{1\perp} \frac{d^3\sigma(\gamma p \rightarrow e^+ X)}{dp_{1\perp} dx_1 d\phi_1} \simeq \frac{8Z^2\alpha^3}{p_{1\perp}^2} \left[(x_1^2 + x_2^2) \left(\log \frac{2x_1 x_2 \omega}{m} - \frac{1}{2} \right) + x_1 x_2 \right]. \quad (61)$$

In the kinematics of Eq. (19) with $p_{1\perp} \simeq Q/2 \simeq 50$ MeV, the rhs of Eq. (61) is equal to $1.7 \mu\text{b}$, leading to a counting rate of 10^3 s^{-1} .

The reaction (44) generates azimuthally symmetric pairs which dilute all the asymmetries. However, the distribution is less peaked at small total transverse momentum $q_\perp = |\mathbf{p}_{1\perp} + \mathbf{p}_{2\perp}|$ than in the case of BH pairs. The decay of relativistic pions in flight, $\pi^0 \rightarrow e^+ e^- \gamma$, yields pairs distributed in the invariant mass W , the total energy ω' , and the relative energies $x_i = \varepsilon_i / \omega'$ according to

$$\frac{d\Gamma(\pi^0 \rightarrow e^+e^-\gamma)}{\Gamma(\pi^0 \rightarrow \gamma\gamma)} \simeq \frac{\alpha}{\pi} (1-\eta)^2 \frac{dW^2}{W^2} \frac{d\omega'}{\varepsilon_\pi} (x_1^2 + x_2^2) dx_1, \quad (62)$$

where ε_π is the pion energy, $\eta = W^2/m_\pi^2$, and $\eta\varepsilon_\pi < \omega' < \varepsilon_\pi$. Since the internal transverse momentum of the pair, $p_{\text{int}} = (m_\pi/\varepsilon_\pi)\sqrt{(\omega' - \eta\varepsilon_\pi)(\varepsilon_\pi - \omega')}$ $\leq (1-\eta)m_\pi/2$, is smaller than the pion momentum, we neglect the effect of p_{int} on the angular distribution of the pairs. Folding the differential cross section $d^2\sigma(\omega, \varepsilon_\pi, \theta)/d\varepsilon_\pi d\Omega_{\text{lab}}$ of inclusive π^0 photoproduction with the photon beam spectrum $I_\gamma d\omega/\omega$ and the decay distribution (62), we find the cross section $\sigma_{\text{backgr}} d\omega'/\omega'$ for producing a pair of energy ω' and central angle $\theta \simeq Q/\omega'$ by photons with energies between ω' and ω_{max} ,

$$\begin{aligned} \sigma_{\text{backgr}} \equiv & 2\pi W Q \frac{d^4\sigma_{\text{back}}}{dW dQ dx_1 d\phi_1} \simeq 4\alpha\omega'\theta^2 (1-\eta)^2 (x_1^2 + x_2^2) \\ & \times \int_{\omega'}^{\omega_{\text{max}}} \frac{d\omega}{\omega} \int_{\omega'}^{\min(\omega'/\eta, \omega)} \frac{d^2\sigma(\omega, \varepsilon_\pi, \theta)}{d\varepsilon_\pi d\Omega_{\text{lab}}} \frac{d\varepsilon_\pi}{\varepsilon_\pi}. \end{aligned} \quad (63)$$

As a numerical example, we consider the case of $\omega' = 600$ MeV, $W = 50$ MeV, $Q = 100$ MeV, $x_1 = x_2 = 0.5$, and $\omega_{\text{max}} = 900$ MeV. Using the unpolarized differential cross section $d\sigma/d\Omega_{\text{lab}} \simeq 2 \mu\text{b}/\text{sr}$ of the exclusive reaction $\gamma p \rightarrow \pi^0 p$ at $\theta \simeq 9.5^\circ$ as a substitute for the inclusive one, we obtain $\sigma_{\text{backgr}} = 0.20$ nb.

V. SUMMARY

Recently, virtual Compton scattering off the nucleon has attracted considerable interest (for an overview see [24]). At low energies, the so-called generalized polarizabilities [26] are accessible in the reaction $e^-p \rightarrow e^-p\gamma$, whereas investigations at high energies allow one to study the wave function of the valence quarks in the nucleon [27]. On the other hand, photoproduction of lepton pairs in the reaction $\gamma p \rightarrow pe^+e^-$ has been proposed to test vector meson dominance for the nucleon [28], to obtain information on the time-like form factors of the nucleon [28–30], and to investigate the longitudinal response of resonances [30].

In this work we have suggested to study pair production for yet another reason. We have argued that small-angle photoproduction of e^+e^- pairs may be used to measure the forward scattering amplitude of real photons. The mechanism which makes such investigations possible is an interference between the Bethe-Heitler amplitude and the virtual Compton scattering amplitude leading to an asymmetry between the electron and positron angular distributions. A determination of the real and imaginary parts of f_1 and f_2 requires a longitudinally polarized target and circularly polarized photons. The imaginary part of f_2 , which is of particular importance for testing the validity of the Gerasimov-Drell-Hearn sum rule, can be measured with target polarization only.

We have proposed specific kinematical conditions which would be particularly appropriate for a determination of f_2 . The uncertainties due to a longitudinal photon polarization, finite photon mass, and the emission of the virtual photon at small non-forward angles have been estimated. We have argued that for the kinematics proposed the corresponding errors are small. Our estimate has also shown that possible backgrounds, essentially from π^0 decays, give rise to small effects only.

In conclusion, photoproduction of e^+e^- pairs provides a possibility to determine the real-photon forward scattering amplitude. In particular, this process may be regarded as an alternative to proposed experiments to test the Gerasimov-Drell-Hearn sum rule by cross section measurements.

ACKNOWLEDGMENTS

A.L. thanks the theory group of the Institut für Kernphysik and the SFB 201 for their hospitality and support during his stay in Mainz where a part of this work was done. S.S. thanks the TMR programme of the European Commission ERB FMRX-CT96-008 for partial financial support.

APPENDIX A: REAL COMPTON SCATTERING AT NON-FORWARD ANGLES

In terms of the invariant amplitudes $A_i(\omega, t)$ [14] the amplitude for real Compton scattering has the following form in the lab frame:

$$\begin{aligned}
T_{\text{CS}} = \frac{\omega\omega'}{N(t)} & \left\{ 2M\boldsymbol{\epsilon}'^* \cdot \boldsymbol{\epsilon} \left[N^2(t)(-A_1 - A_3) - \frac{\nu^2}{M^2}A_5 - A_6 \right] \right. \\
& + 2M\mathbf{s}'^* \cdot \mathbf{s} \left[N^2(t)(A_1 - A_3) + \frac{\nu^2}{M^2}A_5 - A_6 \right] \\
& - 2i\nu\boldsymbol{\sigma} \cdot \boldsymbol{\epsilon}'^* \times \boldsymbol{\epsilon} (A_5 + A_6) + 2i\nu\boldsymbol{\sigma} \cdot \mathbf{s}'^* \times \mathbf{s} (A_5 - A_6) \\
& + i\boldsymbol{\sigma} \cdot \mathbf{k} \mathbf{s}'^* \cdot \boldsymbol{\epsilon} \left[A_2 + \left(1 - \frac{\omega'}{M}\right)A_4 + \frac{\nu}{M}A_5 + A_6 \right] \\
& - i\boldsymbol{\sigma} \cdot \mathbf{k}' \boldsymbol{\epsilon}'^* \cdot \mathbf{s} \left[A_2 + \left(1 + \frac{\omega}{M}\right)A_4 - \frac{\nu}{M}A_5 + A_6 \right] \\
& - i\boldsymbol{\sigma} \cdot \mathbf{k} \boldsymbol{\epsilon}'^* \cdot \mathbf{s} \left[-A_2 + \left(1 - \frac{\omega'}{M}\right)A_4 - \frac{\nu}{M}A_5 + A_6 \right] \\
& \left. + i\boldsymbol{\sigma} \cdot \mathbf{k}' \mathbf{s}'^* \cdot \boldsymbol{\epsilon} \left[-A_2 + \left(1 + \frac{\omega}{M}\right)A_4 + \frac{\nu}{M}A_5 + A_6 \right] \right\}. \tag{A1}
\end{aligned}$$

Here $\omega' = \omega/(1 + (1 - z)\omega/M)$ is the final photon energy, $z = \cos\theta$, $\nu = (\omega + \omega')/2$, $t = -2\omega\omega'(1 - z)$ is the invariant momentum transfer squared, and $N(t) = (1 - t/4M^2)^{1/2}$. The two magnetic vectors \mathbf{s} and \mathbf{s}' are defined as

$$\mathbf{s} = \hat{\mathbf{k}} \times \boldsymbol{\epsilon} = -ih_\gamma\boldsymbol{\epsilon}, \quad \mathbf{s}' = \hat{\mathbf{k}}' \times \boldsymbol{\epsilon}' = -ih'_\gamma\boldsymbol{\epsilon}', \tag{A2}$$

for helical vectors $\boldsymbol{\epsilon}$ and $\boldsymbol{\epsilon}'$ as defined in Eq. (24), with $\boldsymbol{\epsilon}'^* \cdot \boldsymbol{\epsilon} = (1 + h_\gamma h'_\gamma z)/2$.

Since we are interested in no-spin-flip transitions which interfere with the essentially no-spin-flip Bethe-Heitler amplitude T_{BH} , we set $\boldsymbol{\sigma} \rightarrow h_N \hat{\mathbf{k}}$ in the above equation. We have to distinguish two cases:

i) No photon helicity flip ($h'_\gamma = h_\gamma$). In this case the amplitude (A1) becomes

$$T_{\text{CS}} \equiv 8\pi M \left(f_1(\omega, t) - h_\gamma h_N \omega f_2(\omega, t) \right), \tag{A3}$$

where

$$\begin{aligned}
f_1(\omega, t) &= -\frac{(1+z)\omega\omega'}{4\pi N(t)} \left(A_6(\omega, t) + A_3(\omega, t)N^2(t) \right), \\
f_2(\omega, t) &= \frac{(1+z)\omega'^2}{8\pi M N(t)} \left((z-1)A_6(\omega, t) + (z+1)A_4(\omega, t) \right).
\end{aligned}
\tag{A4}$$

At energies ω of a few GeV and small t we may expect that the slope $B/2$ of the amplitude $f_1(\omega, t)$ considered as a function of t follows the diffractive behavior of the differential cross section of Compton scattering, $d\sigma/dt \propto \exp(Bt)$ with $B \simeq 6 \text{ GeV}^{-2}$ [20]. Meanwhile, the high energy behavior of the amplitude f_2 , including its slope, is unknown.

ii) Photon helicity flip ($h'_\gamma = -h_\gamma$). In this case the amplitude vanishes at $t = 0$, and the leading term $O(t)$ is

$$T_{\text{CS}} \equiv 8\pi M \left(\tilde{f}_1(\omega, t) - h_\gamma h_N \omega \tilde{f}_2(\omega, t) \right), \tag{A5}$$

where

$$\begin{aligned}
\tilde{f}_1(\omega, t) &\simeq \frac{t}{8\pi} \left(A_1(\omega, 0) + \frac{\omega^2}{M^2} A_5(\omega, 0) \right), \\
\tilde{f}_2(\omega, t) &\simeq \frac{t}{8\pi M} \left(1 + \frac{\omega}{M} \right) A_5(\omega, 0).
\end{aligned}
\tag{A6}$$

The high-energy behavior of the helicity-flip amplitudes is also unknown. As discussed in [14], data on electromagnetic polarizabilities of the nucleon put some constraints on the amplitude $A_1(\omega, 0)$.

In the energy region below $\simeq 1 \text{ GeV}$, the amplitudes A_i are dominated by nucleon resonances, other known channels of the nucleon photoexcitation, and a few t -channel exchanges (mostly π^0 and σ). Using unitarity, dispersion relations, and plausible assumptions on the high-energy behavior of the amplitudes A_1 and A_2 , one can determine all the A_i and describe the available data on Compton scattering with *unpolarized* and *single-polarized* particles [14]. Using these results as they are, we find all the amplitudes f_1 , f_2 , \tilde{f}_1 , and \tilde{f}_2 through (A4), (A6) and directly estimate their t -dependence.

REFERENCES

- [1] S.B. Gerasimov, *Sov. J. Nucl. Phys.* **2**, 430 (1966).
- [2] S.D. Drell and A.C. Hearn, *Phys. Rev. Lett.* **16**, 908 (1966).
- [3] D. Drechsel, *Prog. Part. Nucl. Phys.* **34**, 181 (1995).
- [4] S.D. Bass, *nucl-th/9703254*, 1997.
- [5] F.E. Low, *Phys. Rev.* **96**, 1428 (1954).
- [6] M. Gell-Mann and M.L. Goldberger, *Phys. Rev.* **96**, 1433 (1954).
- [7] P.D.B. Collins, “An Introduction to Regge Theory and High Energy Physics”, Cambridge University Press (1977).
- [8] G.C. Fox and D.Z. Freedman, *Phys. Rev.* **182**, 1628 (1969).
- [9] I. Karliner, *Phys. Rev. D* **7**, 2717 (1973).
- [10] R.L. Workman and R.A. Arndt, *Phys. Rev. D* **45**, 1789 (1992).
- [11] V.D. Burkert and Z. Li, *Phys. Rev. D* **47**, 46 (1993).
- [12] A.M. Sandorfi, C.S. Whisnant, and M. Khandaker, *Phys. Rev. D* **50**, R6681 (1995).
- [13] R.A. Arndt, I.I. Strakovsky, and R.L. Workman, *Phys. Rev. C* **53**, 430 (1996), and the code SAID.
- [14] A.I. L’vov, V.A. Petrun’kin, and M. Schumacher, *Phys. Rev. C* **55**, 359 (1997).
- [15] H. Alvensleben et al., *Phys. Rev. Lett.* **30**, 328 (1973).
- [16] M. Jacob and G.C. Wick, *Ann. Phys.* **7**, 404 (1959).
- [17] Y. Hara, *Progr. Theor. Phys. Suppl.* **51**, 96 (1972).
- [18] R.A. Berg and C.N. Lindner, *Nucl. Phys.* **26**, 259 (1961).
- [19] J.A. Gómez Tejedor and E. Oset, *Nucl. Phys.* **A571**, 667 (1994).
- [20] J. Duda et al., *Z. Phys. C* **17**, 319 (1983).
- [21] A.I. L’vov, S. Scopetta, D. Drechsel, and S. Scherer, *nucl-th/9607004*, 1996. Also in *Proc. Workshop on Virtual Compton Scattering, Clermont-Ferrand, June 1996*, ed. V. Breton.
- [22] M. Mac Cormick et al., *Phys. Rev. C* **53**, 41 (1996).
- [23] T.A. Armstrong et al., *Phys. Rev. D* **5**, 1640 (1972).
- [24] *Proc. Workshop on Virtual Compton Scattering, Clermont-Ferrand, June 1996*, ed. V. Breton.
- [25] R.L. Gluckstein and M.H. Hall, Jr., *Phys. Rev.* **90**, 1030 (1953).
- [26] P.A.M. Guichon, G.Q. Liu, and A.W. Thomas, *Nucl. Phys.* **A591**, 606 (1995).
- [27] P. Kroll, M. Schürmann, and P.A.M. Guichon, *Nucl. Phys.* **A598**, 435 (1996).
- [28] M. Schäfer, H.C. Dönges, and U. Mosel, *Phys. Lett. B* **342**, 13 (1995).
- [29] A.E.L. Dieperink and S.I. Nagorny, *Phys. Lett. B* **397**, 20 (1997).
- [30] A.Yu. Korchin, O. Scholten, and F. de Jong, *Phys. Lett. B* **402**, 1 (1997).

FIGURE CAPTIONS

Fig. 1: Kinematics of the reaction $\gamma N \rightarrow e^+e^-N'$. The kinematical variables are described in the text.

Fig. 2: Diagrams contributing to lepton pair production: Bethe–Heitler mechanism (left) and virtual Compton scattering (right).

Fig. 3: The Bethe–Heitler cross section (46) for the proton as a function of the invariant mass W of the pair at incident photon energy $\omega=1000$ MeV, azimuthal angle $\phi_1 = 90^\circ$, $x_1 = x_2 = 0.5$, and for three values of 4-momentum transfer, $Q = 75$ MeV (dashed curve), $Q = 100$ MeV (full curve), and $Q = 125$ MeV (dotted curve).

Fig. 4: The real and imaginary parts of the no-spin-flip and spin-flip amplitudes f_1 and f_2 , respectively, as functions of the beam energy ω . The calculations are described in the text.

Fig. 5: The four asymmetries A_γ , A_N , A and $A_{\gamma N}$ as functions of the beam energy ω , at fixed value of the invariant mass of the pair, $W = 50$ MeV, and at $x_1 = x_2 = 0.5$. Dashed curve: $Q = 75$ MeV, full curve: $Q = 100$ MeV, dotted curve: $Q = 125$ MeV.

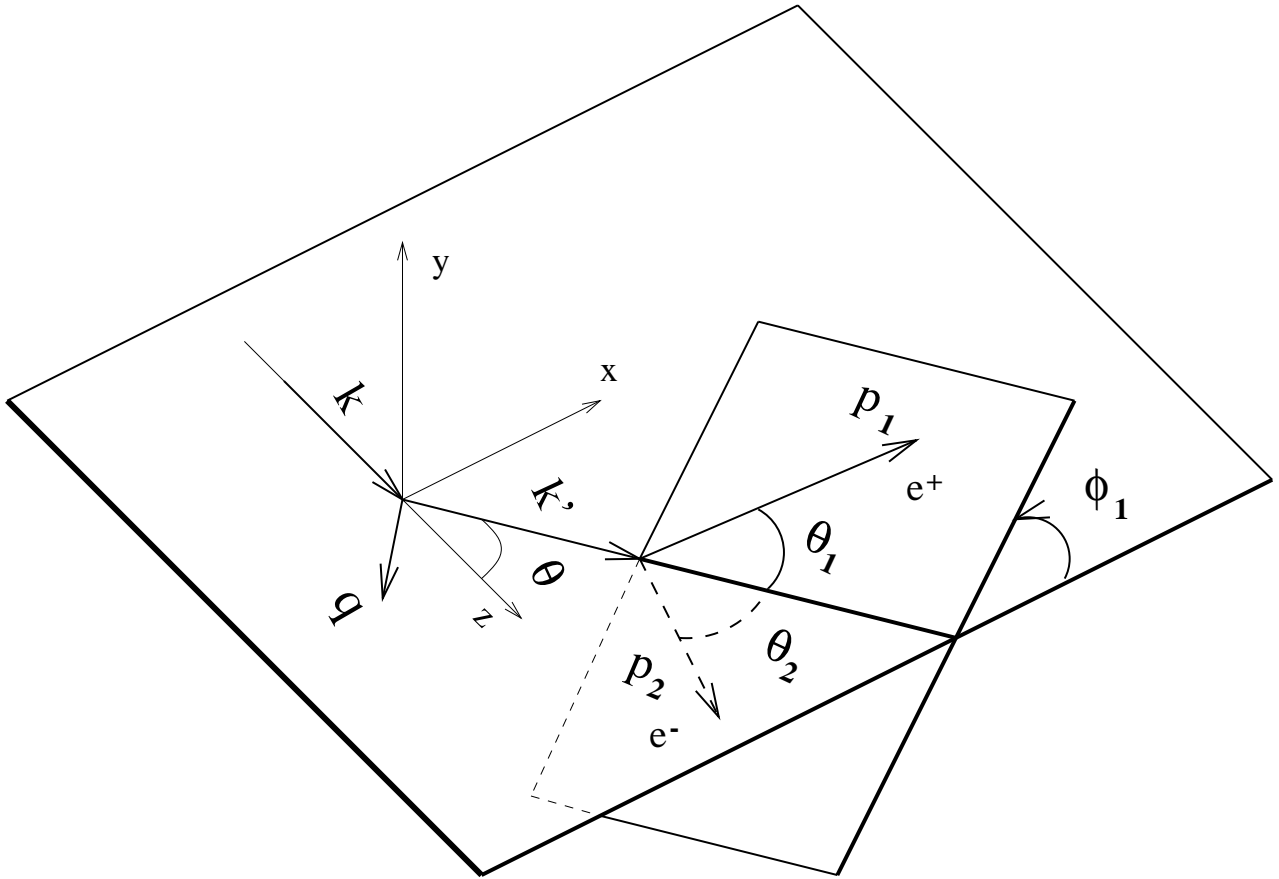
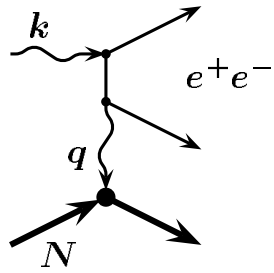
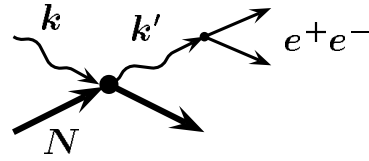


FIGURE 1



BH



VCS

FIGURE 2

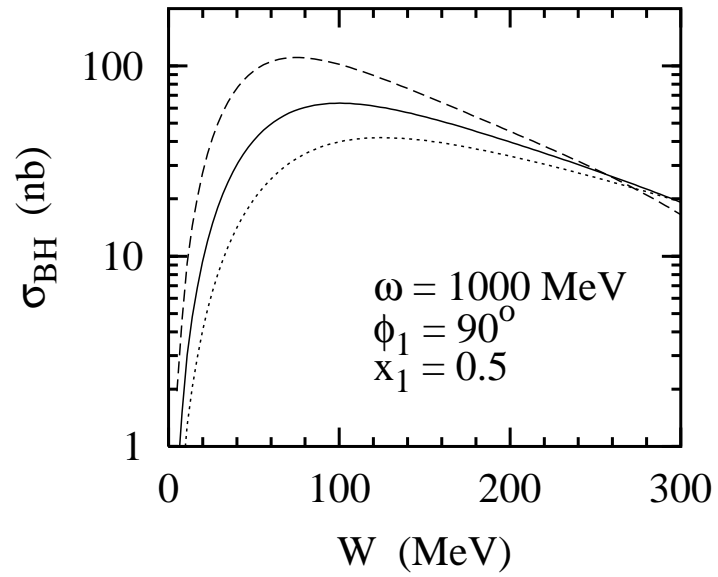


FIGURE 3

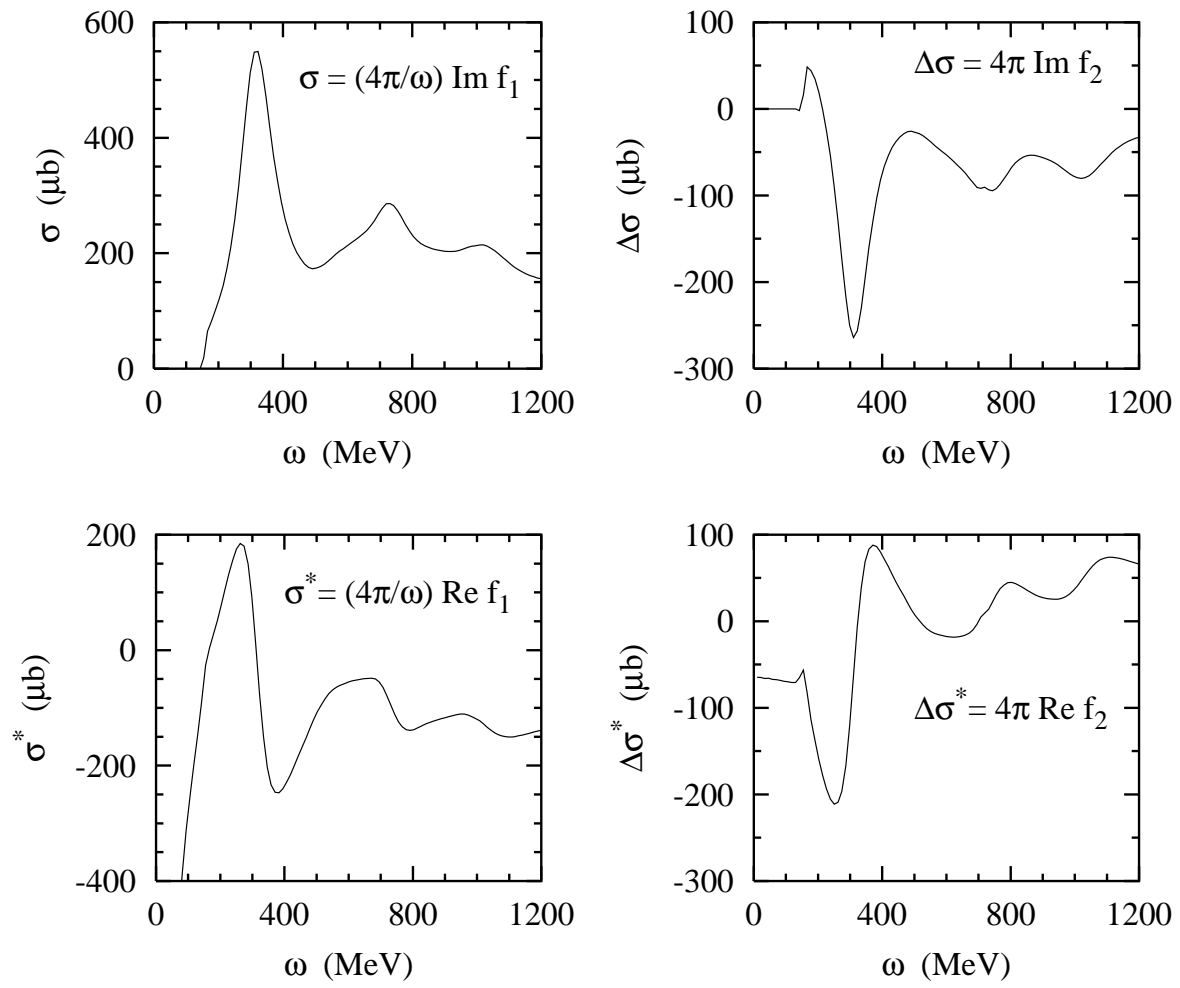


FIGURE 4

$W = 50 \text{ MeV}, x_1 = 0.5$

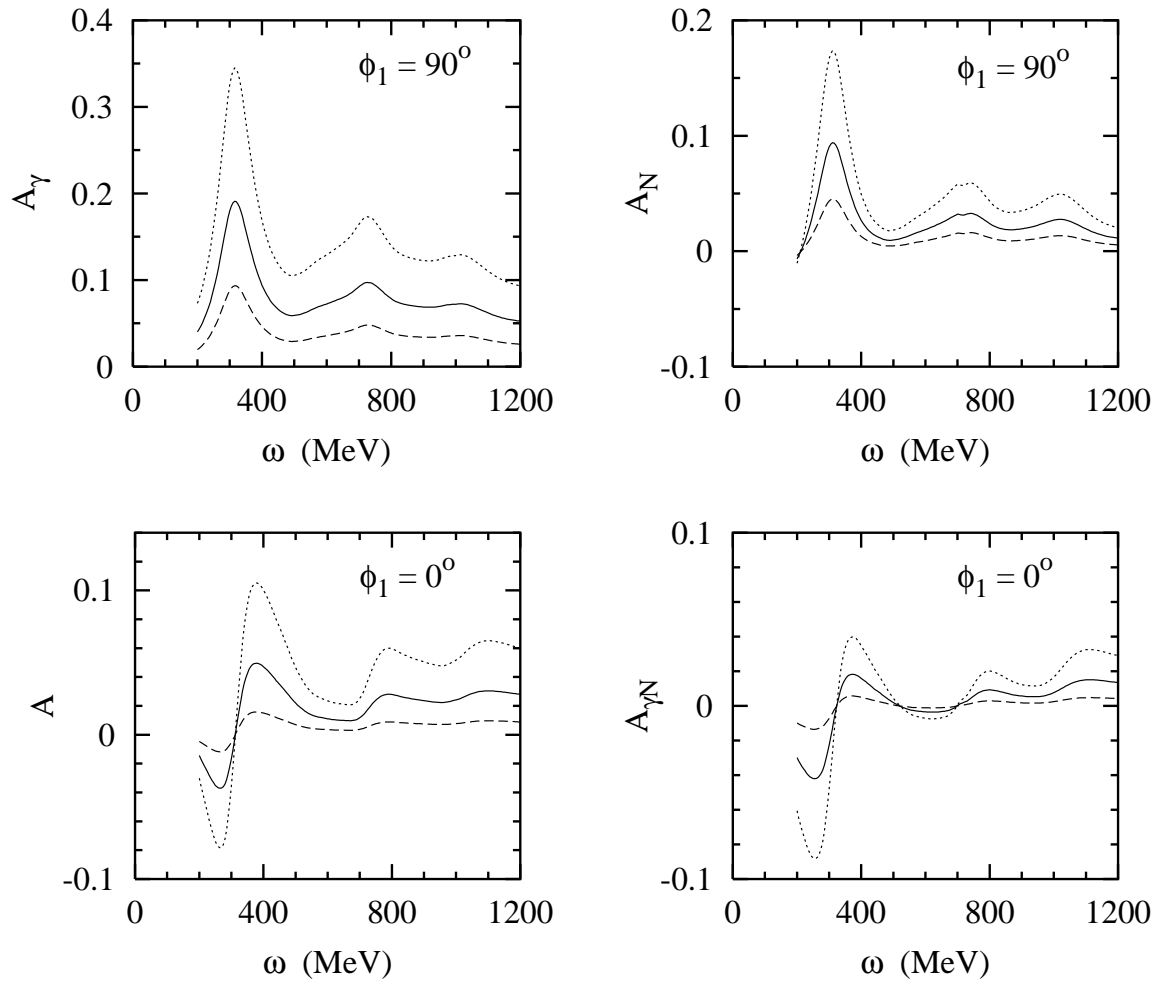


FIGURE 5